Signatures of critical behavior in the multifragmentation of nuclei with charge $Z = 12$–15 and the N/Z dependence

M. Jandel, S. Wuenschel, D. V. Shetty, G. A. Souliotis, A. L. Keksis, and S. J. Yennello
Cyclotron Institute, Texas A&M University, College Station, Texas 77843, USA

M. Veselsky
Institute of Physics, Slovak Academy of Sciences, Dubravska cesta 9, Bratislava, Slovakia
(Received 21 February 2006; published 22 November 2006)

We have investigated the disassembly of light nuclear systems with charge 12–15 to extract the power-law parameters of the fragmenting nuclear system. Excited nuclei were produced in semiperipheral reactions ^{28}Si + ^{112,124}Sn at 30 and 50 MeV/nucleon and the residual cold fragments were detected by the multidetector array for charged particles FAUST. We have studied the power-law parameter τ as a function of the excitation energy of quasiprojectiles. We observe a systematic occurrence of the minimum of τ with respect to the excitation energy accompanied by the maximum of the second moment of the charge distribution in the same region of excitation energy. The main features observed in the characteristics of mass and charge distributions for multifragmentation of heavier systems, such as power-law behavior of charge distribution, are thus observed also for very light systems. Moreover, behavior of the charge distribution with respect to the N/Z degree of freedom has been shown.

DOI: 10.1103/PhysRevC.74.054608 PACS number(s): 25.70.Mn, 25.70.Pq, 25.70.Lm

I. INTRODUCTION

The relation between nuclear multifragmentation and the liquid-gas-type phase transition was first suggested by the observation that the mass distribution of fragmentation products from an experiment [1,2] closely resembled the power-law prediction of Fisher's droplet model [3]. Since then, experimental work in this direction has progressed tremendously with improving beam facilities and detector setups and the search for the nuclear liquid-gas phase transition in reactions induced by heavy-ion and light-ion beams at intermediate and high energies has been documented in numerous works [4–24]. Signals of the liquid-gas phase transition in terms of critical exponents were studied in many systems [6,10,14–16,20,25–27]. As pointed out by Natowitz *et al*. [28], the apparent critical behavior in the fragmentation of heavier nuclei ($A > 60$) is influenced by finite-size effects or the growth of fluctuations in the spinodal region [29,30]. It has been argued [28] that because of smaller Coulomb effects for systems with $A < 60$, the critical behavior in such systems can be observed. Evidence of a nuclear liquid-gas phase transition in small systems ($A \sim 36$) has been recently reported [31], and critical exponents as a function of the temperature of the source and their behavior have been confirmed by several theoretical models. As was shown in [31], both the lattice gas model [32,33] and classical molecular dynamics [34] show that the minimum of the critical exponents τ and λ and the maximum of the normalized second moment of the charge distribution, S_2, are reached in the vicinity of the critical point, in agreement with experimental observations [31].

In a time-scale study [35], the time for the initial breakup of quasiprojectiles in peripheral reactions of ^{28}Si + ^{112,124}Sn at 30 and 50 MeV/nucleon was found to be less than 30–50 fm/c for excitation energies higher than 4 MeV/nucleon. This indicates a rapid (almost simultaneous) breakup of a highly excited quasiprojectile. The simultaneous breakup is a necessary supposition to study the possible critical behavior of small nuclear systems, as also mentioned in [36].

In this work we present an analysis of the fragmentation of quasiprojectiles in ^{28}Si + ^{112,124}Sn reactions at 30 and 50 MeV/nucleon [37]. We will extract the power-law parameter τ and the second moment of the charge distribution, S_2, as well as their dependence on the N/Z degree of freedom. The experiment is briefly described in Sec. II. In Sec. III A, the measured charge distributions are shown in terms of the power-law parameter τ and moments of charge distributions. In Sec. III B, the statistical multifragmentation model is used to describe the experimental observables and the primary charge distributions. In Sec. III C, the power-law parameter τ is extracted by using the correlations between higher moments of the charge distribution. The N/Z degree of freedom and its effect on the charge distribution is investigated in Sec. III D. Finally, the results are summarized and discussed in Sec. IV.

II. EXPERIMENT

The experiment was carried out at the Texas A&M Cyclotron Institute, where reactions of ^{28}Si + ^{112,124}Sn at 30 and 50 MeV/nucleon were studied. Details of the experimental setup can be found in Ref. [37]. Charged particles were detected by the multidetector array FAUST [38]. The apparent excitation energy of the quasiprojectile was obtained by using the calorimetric relation

$$E^*_{\rm app} = \sum_i \left(\Delta m_i + T_i^{\rm PLS}\right) - \Delta M_{\rm PLS}, \qquad (1)$$

where $T_i^{\rm PLS}$ are the kinetic energies of the fragments in the center of mass of the projectile-like source, Δm_i are the

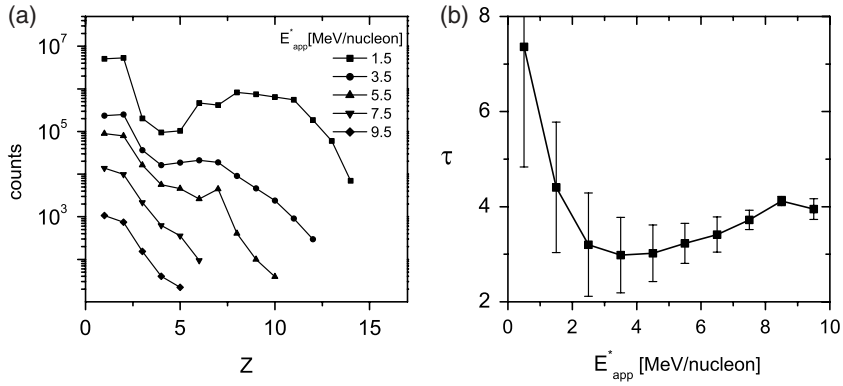

FIG. 1. (a) Charge distribution of the fragments from Si + Sn reactions with reconstructed quasiprojectiles of charge $Z(\mathrm{QP}) = 12$–15. Different symbols show the charge distributions for different bins of quasiprojectile excitation energy. (b) Values of τ obtained by fitting the charge distributions with a power-law function.

mass excesses of the fragments, and ΔM_{PLS} is the mass excess of the projectile-like source. No free neutrons were detected. Previous analysis of these experimental data [39] only included the events corresponding to isotopically resolved fragments ($Z \leqslant 5$) detected by the FAUST array with a total reconstructed quasiprojectile charge of $Z_{\mathrm{tot}} = 12$–15. It was shown that these events originated predominantly from the multifragmentation of the projectile-like fragment. In this work we include isotopically unresolved fragments ($Z > 5$) as well. The mass assigned to these fragments in the off-line analysis was that of the most stable isotope for the given charge. This introduces an error in the determination of the excitation energy of the quasiprojectile, mainly in the low-excitation-energy region. Comparing the experimental data with theoretical calculation, we find that this error can be as much as 15% in the region of 1–3 MeV/nucleon. However, this error has no significant impact on the overall analysis and or on the results presented. To exclude the events where pre-equilibrium or midrapidity particles were detected (with $Z \leqslant 2$), the total velocity of particles in the center-of-mass reference frame was constrained to be $v < 0.2c$. In this analysis, we summed the events from all four reactions that were measured. The reconstructed quasiprojectiles obtained from different reactions are independent of the reaction from which they were formed [39]. We checked this fact by independently constructing the charge distributions for the same excitation energy bins in all four reactions, and values of τ differed by less than $\Delta\tau < 0.3$.

III. RESULTS

A. Evolution of the charge distribution

The charge distributions as a function of the quasiprojectile (QP) excitation energy for the charge 12–15 from ^{28}Si + ^{112,124}Sn reactions at 30 and 50 MeV/nucleon are shown in Fig. 1(a). At low excitation energies, a characteristic U-shaped distribution with an exponential fall is observed. The appropriate way to describe the charge distributions and look for an apparent connection to the critical behavior is to fit the charge distributions with a power-law function $n(Z) \sim Z^{-\tau}$, where the coefficient τ is a power-law parameter. At the critical point, phases are indistinguishable and the size distribution should obey the power law. Similarly to Ma *et al.* [31], we fitted the charge distribution in the interval $Z = 2$–5. In Fig. 1(b), the values of τ are shown for the distributions shown in Fig. 1(a). The fit is not good in the region of low excitation energies, giving large error bars on the power-law parameter τ. In the region of 3–5 MeV/nucleon we observe that the τ parameter begins to increase with increasing excitation energy E^*_{app}, which may signal the existence of a minima in that region of E^*_{app}. At an excitation energy $E^*_{\mathrm{app}} \sim 4$ MeV/nucleon the value of τ is $\tau_{\mathrm{min}} = 2.9 \pm 0.6$.

The second moment of the charge distribution, S_2, as a function of the excitation energy is shown in Fig. 2. The analysis was performed with the data including quasiprojectiles with the charge $Z(\mathrm{QP}) = 12$–15 and the S_2 behavior is shown by a thick line. Exclusive data with the fixed quasiprojectile charge $Z(\mathrm{QP}) = 12, 13, 14,$ and 15 were also analyzed. Different symbols and lines represent different $Z(\mathrm{QP})$ according to the legend of Fig. 2. The S_2 dependence on the excitation energy clearly shows a maximum in the excitation energy region

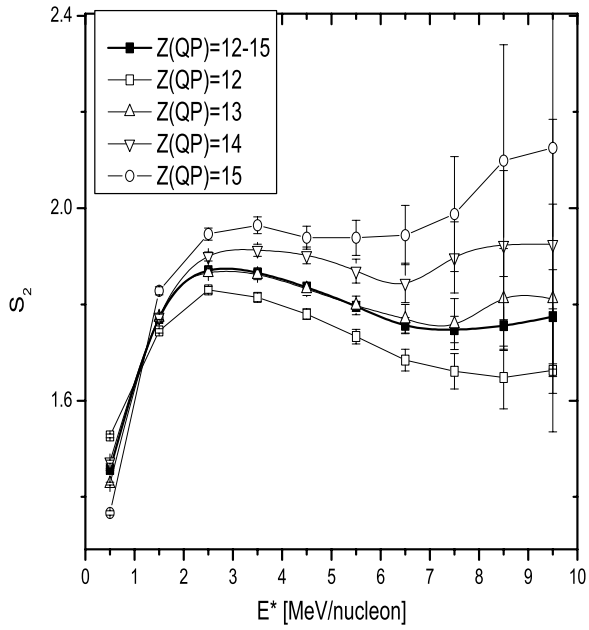

FIG. 2. The second moment of the charge distribution, S_2, as a function of excitation energy of the QP. The thick line and the full squares show inclusive data on the reconstructed QP with charges $Z(\mathrm{QP}) = 12$–15. Different symbols represent S_2 for exclusive data on $Z(\mathrm{QP}) = 12, 13, 14,$ and 15.

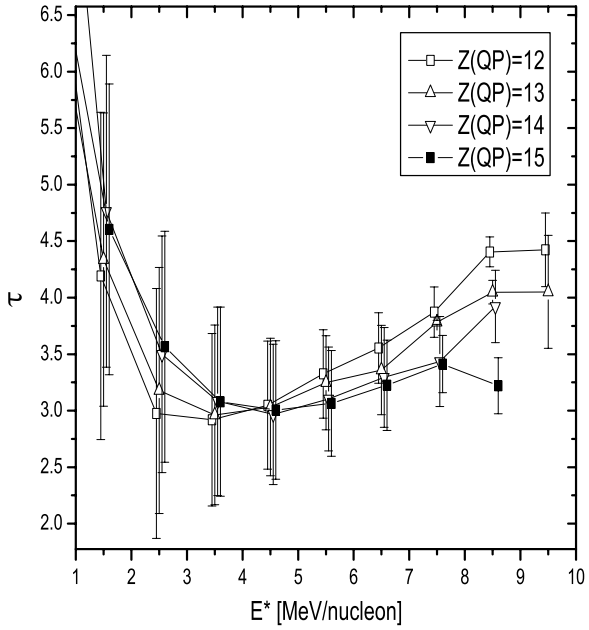

FIG. 3. Exponent τ as a function of the apparent excitation energy obtained for $Z(\mathrm{QP}) = 12$, 13, 14, and 15.

$E^* \sim 3$–4 MeV/nucleon. The dependence of quasiprojectile size is also seen, as the absolute value of S_2 increases with increasing quasiprojectile charge. Similarly, the transition point, where S_2 shows a maximum, slightly increases with increasing quasiprojectile charge. In the same manner, τ was analyzed for the fixed quasiprojectiles charge $Z(\mathrm{QP}) = 12$, 13, 14, and 15. The results are shown in Fig. 3. The transition energy, where the τ value reaches its minimum, appears to increase with increasing size of the system and the absolute value is approximately constant at $\tau_{\min} = 2.9$–3.0. Given the size of the error bars, the deviations of τ as a function of the size of the system are indistinguishable; therefore the dependence of the power-law parameter τ needs further investigation to draw more definite conclusions.

As was shown in previous work [31–34], the appearance of the extrema may signal a liquid-gas transition in finite systems. In the present work, we observe a signal that may support this hypothesis in terms of the maximum found in the S_2 dependence on the excitation energy. The τ is suggestive of the dependence on the excitation energy but is less conclusive owing to the rather large errors in the power-law fits. This region of excitation energies is where multifragmentation starts to play an important role in the exit channel and thus the behavior of S_2 and τ may reflect the transition of the mechanism from evaporation to multifragmentation, as a result of an increased phase space in the exit channel.

B. Comparison with theoretical prediction

Up to this point, we have dealt with the measured charge distributions, which do not reflect exactly the charge distributions at the instant of breakup of the quasiprojectile because of the de-excitation of hot primary fragments. There is no model-independent way to determine the charge distributions of primary fragments at the moment of breakup. In this section we will describe the method for determining the primary breakup partitions by using theoretical models and obtaining the primary charge distributions. A peripheral nuclear reaction at incident energies of 30–50 MeV/nucleon can be divided into three stages. The first stage is the formation of the quasiprojectile. For this stage, we employed the deep inelastic transfer (DIT) model of Tassan-Got [40]. The second stage is the fragmentation of the quasiprojectile. The calculation of primary hot fragments was performed using the statistical multifragmentation model (SMM) [41,42]. The de-excitation of primary products through statistical emission and Fermi breakup was calculated by using the evaporation code embedded in the SMM code [43]. All the simulation results were filtered using a software replica of the FAUST array, and these were then compared to the experimental values. The software filter takes into account the energy thresholds of detected particles and the exact geometry of the FAUST setup. No significant discrepancies between filtered and unfiltered events were observed.

We performed all three stages of the calculation for the reaction $^{28}\mathrm{Si} + {}^{112}\mathrm{Sn}$ at 50 MeV/nucleon and compared the results with the corresponding experimental data for this reaction. Primary and secondary mass distributions of the quasiprojectiles with charge $Z = 14$ from the reaction $^{28}\mathrm{Si} + {}^{112}\mathrm{Sn}$ at 50 MeV/nucleon are shown in Fig. 4. The primary distribution obtained from the DIT calculation was used as an input to the SMM code. The experimental mass distribution is also compared to the calculated one in Fig 4. The secondary

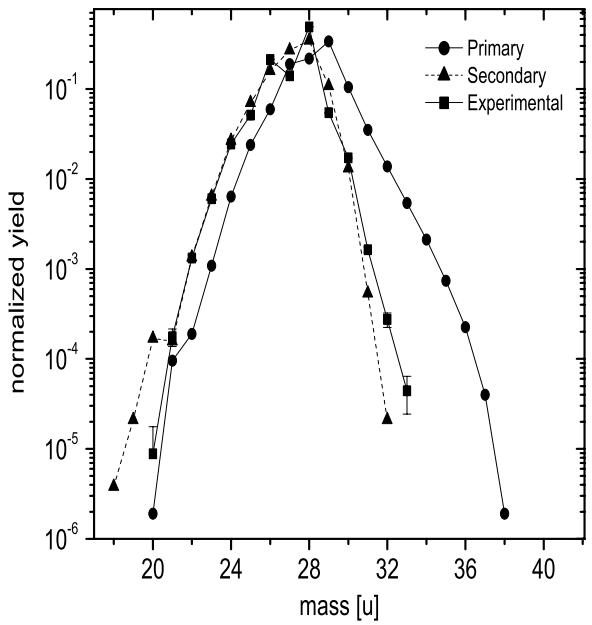

FIG. 4. The mass distribution of the quasiprojectiles obtained by DIT simulation from the reaction $^{28}\mathrm{Si} + {}^{112}\mathrm{Sn}$ at 50 MeV/nucleon (circles). Measured and simulated (DIT-SMM) reconstructed quasiprojectile mass distribution are shown by squares and triangles, respectively.

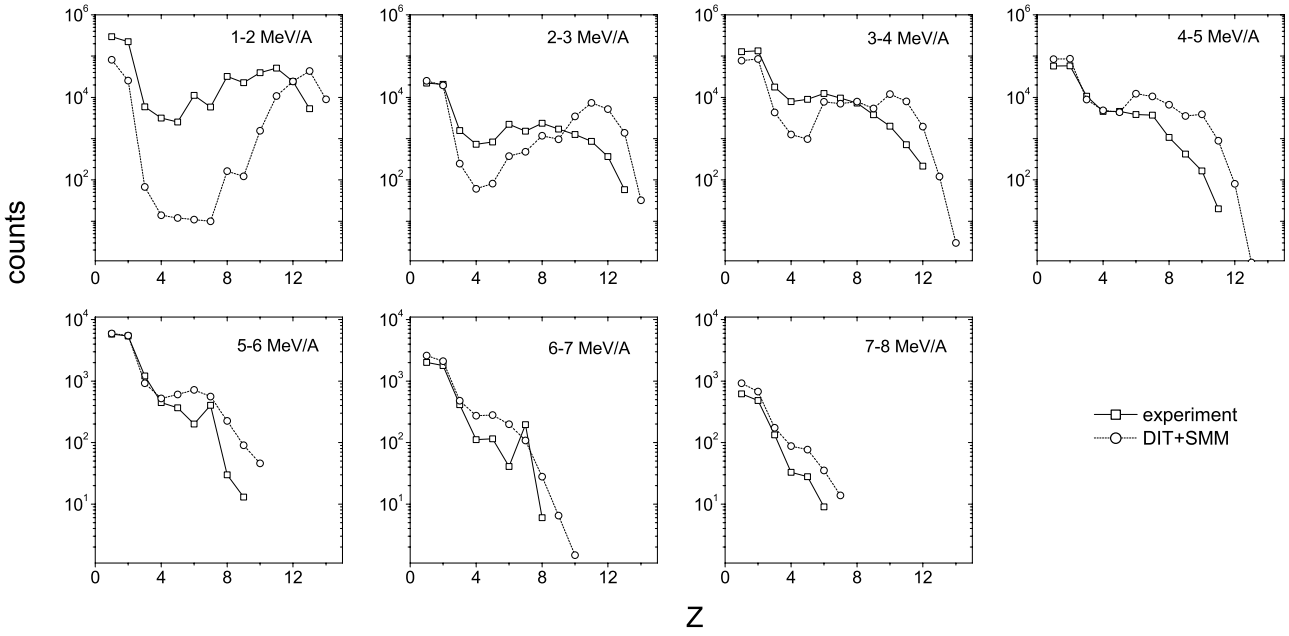

FIG. 5. Measured charge distribution for different bins of QP excitation energy (squares) and the charge distribution of fragments obtained from coupled DIT-SMM calculations (circles).

mass distribution was obtained by summing the mass number of all fragments except neutrons, event by event. Agreement is achieved to a high degree of accuracy in the whole mass region except for masses $A < 21$ and $A > 31$.

A more detailed comparison of experimental and calculated data is shown in Fig. 5, where we compare charge distributions of fragments arising from the disassembly of quasiprojectiles with the charge $Z(\mathrm{QP}) = 14$ in the reaction $^{28}\mathrm{Si} + ^{112}\mathrm{Sn}$ at 50 MeV/nucleon, exclusively. The charge distribution was compared for several excitation energy bins of quasiprojectiles from 0.5 to 9.5 MeV/nucleon. Experimental and simulated charge distributions were fitted to obtain τ values. In Fig. 6, the dependence of τ on the excitation energy is shown for experimental and calculated charge distributions. The parameter τ as a function of excitation energy has the same behavior for calculated and measured secondary fragments, with a minimum at $\sim$5 MeV/nucleon. The $\tau_{\mathrm{min}} = 1.6\pm0.5$ for secondary fragments obtained from the simulation is however significantly lower than $\tau_{\mathrm{min}} = 2.9\pm0.6$ obtained from the experimental data. The charge distributions of primary hot fragments have a more pronounced parabolic shape than the secondary fragment charge distribution and the minimum is located at excitation energy $\sim$5.5 MeV/nucleon, similar to secondary fragments. The value of the power-law parameter $\tau_{\mathrm{min}} = 0.6\pm0.2$ for primary fragments compared to the $\tau_{\mathrm{min}} = 1.6\pm0.5$ value obtained for secondary fragments from our calculation shows that the secondary emission plays an important role in the framework of our model.

For comparison, the values of τ obtained from a classical molecular dynamics model are also shown in Fig. 6. Details of this calculation are given in the appendix. By this simple dynamical calculation we obtained very similar results for τ values compared to the measured ones. The minimum of τ is located at $E^* \sim 4.5$ MeV/nucleon.

C. N/Z degree of freedom

Isospin asymmetry may play a significant role in the breakup of hot nuclei [47–49]. The critical temperature is suggested to be lower for systems with N/Z away from $N/Z = 1$. Moreover, as outlined in [49], typical van der Waals

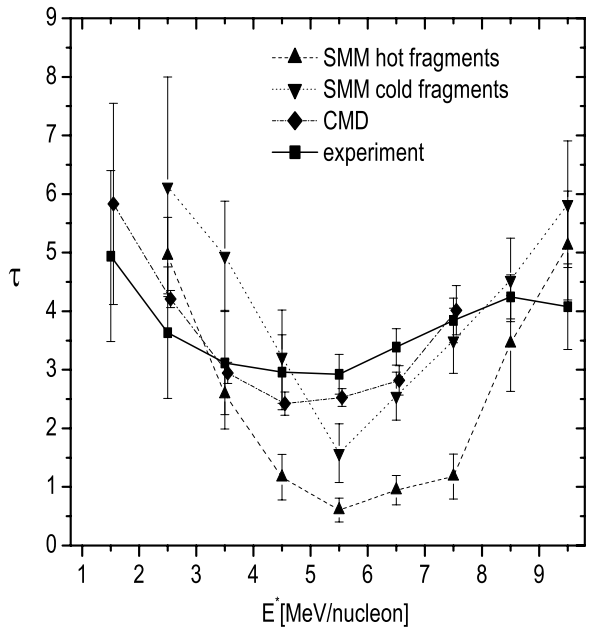

FIG. 6. τ values for the primary and the secondary charge distributions as a function of the excitation energy of QP. A comparison of different theoretical models with the experimental data is shown by different symbols; empty squares connected by dashed lines represent inclusive $Z(\mathrm{QP}) = 14$ data and empty triangles connected by full lines show results from $^{28}\mathrm{Si} + ^{112}\mathrm{Sn}$ at 50 MeV/nucleon reaction.

behavior of the one-component matter at phase transition is not seen in the detailed relativistic mean-field calculation of warm, diluted two-component nuclear matter. The pressure, temperature, density, and concentration of the gas and liquid phases may change during the transition.

We will proceed to investigate the possible effects of the N/Z degree of freedom on the power-law parameter τ, which we obtain by gating on the N/Z intervals of the reconstructed experimental data. The value of N/Z is determined by using the reconstructed mass A and charge Z of the quasiprojectile. The dependence of the exponent τ on the excitation energy for the different initial N/Z of the quasiprojectile is shown in Fig. 7. The excitation energy at which τ reaches its minimum appears to increase with the N/Z of the quasiprojectile. The absolute value of $\tau_{\min}$ in the transition point increases with increasing N/Z, as is shown in Fig. 8. The charge distributions change significantly for different N/Z of the quasiprojectile at the same excitation energy. The transition excitation energy E_C (where τ reaches its minimum) is an increasing function of the N/Z of the quasiprojectile, although we observe the values of $\tau_{\min} > 3.0$ for the proton-rich ($N/Z < 1$) quasiprojectiles. The more neutron rich the quasiprojectile, the more the charge distribution in the transition point approaches the power law with $2 < \tau_{\min} < 3$. The minimum of τ is more pronounced compared to low N/Z bins. We believe these data are consistent with an N/Z dependence in the phase transition. Further investigation is underway.

IV. DISCUSSION

A detailed analysis of the fragment charge distributions produced in the $^{28}\mathrm{Si} + {}^{112,124}\mathrm{Sn}$ reactions at 30 and 50 MeV/nucleon was performed. The disassembly of an excited nuclear system with charge $Z = 12$–15 was studied to search for the signals of critical behavior previously reported for the heavier system of mass $A \sim 36$ [31]. The power-law parameter τ and the second moment of the charge distribution, S_2, were extracted from inclusive data for four reactions with quasiprojectile charge of $Z(\mathrm{QP}) = 12$–15. The values of τ and S_2, as a function of apparent excitation energy, were obtained by fitting the charge distributions of the detected fragments in respective apparent excitation energy bins. Similarly, as was observed in [31], the τ value reaches a minimum (with an absolute value of $\tau = 2.9 \pm 0.6$) at $E^*_{\mathrm{app}} \sim 4$ MeV/nucleon. In this region of E^*_{app}, a maximum in S_2 is observed as well. The same trend in τ and S_2 is also observed for the reconstructed charge of QP fixed at 12, 13, 14, and 15.

To estimate the effects of secondary emission we analyzed exclusively one reaction $^{28}\mathrm{Si} + {}^{112}\mathrm{Sn}$ at 50 MeV/nucleon. The primary fragments were obtained by coupled DIT-SMM calculations, and the power-law parameter τ is significantly lower than the one expected from the percolation model [44–46]. In the framework of the DIT-SMM, the secondary emission changes the charge distributions significantly for the disassembly of such a small system, in contrast to what was observed in [47,48] for heavier nuclei. The study of critical behavior in small nucleonic systems ($A < 30$) (despite that it may be favored by arguments put forward in [28]) is therefore more complicated because it requires very detailed treatment of the secondary processes (e.g., evaporation and Fermi breakup). Even though the signatures of spontaneous breakup or multifragmentation were seen [35,39], the admixture of the sequential processes may be difficult to identify and isolate during the analysis of experimental data. Indeed, as shown in [35], sequential emission of light charged particles are still present in the experimental data up to $E^*_{\mathrm{app}} \sim 4$ MeV/nucleon, which may explain, to some extent, the discrepancies between DIT-SMM calculation and experimental values.

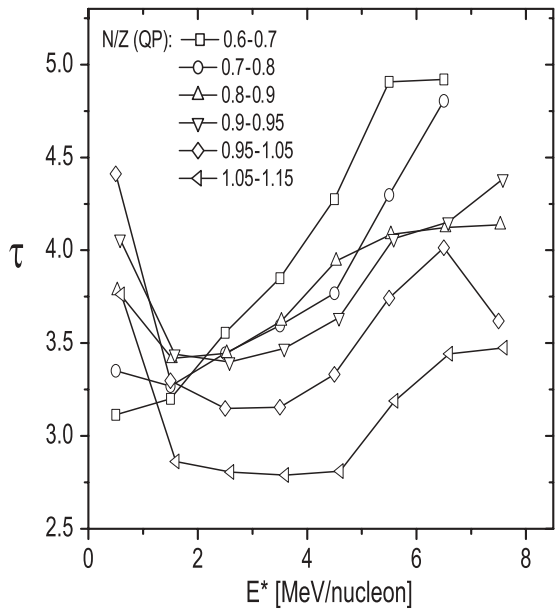

FIG. 7. Exponent τ as a function of excitation energy for different bins in the N/Z of the quasiprojectile.

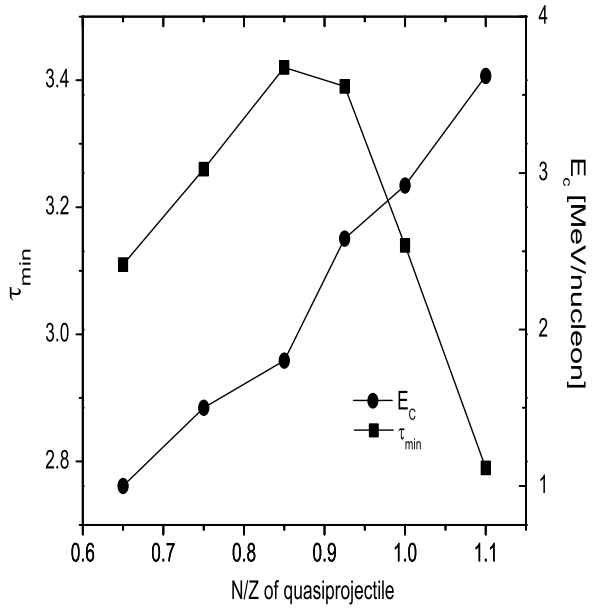

FIG. 8. Exponent $\tau_{\min}$ and transition excitation energy E_C as a function of the N/Z of the quasiprojectile.

The role of isospin asymmetry of the quasiprojectile has been investigated; for fixed N/Z intervals of reconstructed quasiprojectiles, the charge distributions were studied in terms of the power-law parameter τ. To our knowledge, this is the first study of this kind. The results show that the charge distribution is very sensitive to the quasiprojectile N/Z, with $\tau_{\min}$ values having a maximum around $N/Z = 1$. The transition excitation energy E_C increases with increasing quasiprojectile N/Z. Further investigation in this direction is necessary. With the isotopic resolution for particles with $Z > 5$, the role of N/Z in the multifragmentation of reconstructed quasiprojectiles may be extensively studied.

ACKNOWLEDGMENTS

We wish to thank A. Botvina for valuable discussions during the course of this work and J. B. Natowitz for a careful reading of the manuscript and for his comments. We also thank L. Tassan-Got for the DIT model code. This work was supported in part by the Robert A. Welch Foundation through Grant No. A-1266, the Department of Energy through Grant No. DE-FG03-93ER40773, and the Slovak Scientific Grant Agency through Grant No. VEGA-2/5098/25.

APPENDIX

We performed the dynamical calculation of nuclear fragmentation in the classical approximation in the framework of classical molecular dynamics similar to the one in [34]. The model assumes that the nucleons inside the nucleus behave classically and move under the influence of a two-body potential. The form of the isospin-dependent potential was taken from [34,50]:

$$v_{np} = v_r(e^{-\mu_r r}/r - e^{-\mu_r r_c}/r_c) - v_a(e^{-\mu_a r}/r - e^{-\mu_a r_c}/r_c), \quad \text{(A1)}$$

$$v_{nn} = v_{pp} = v_0(e^{-\mu_0 r}/r - e^{-\mu_0 r_c}/r_c). \quad \text{(A2)}$$

A ground-state configuration was established by minimization of potential energy by moving particles inside a sphere of radius $R = 1.18A^{1/3}$. Afterward, the momenta of nucleons were assigned by assuming a Maxwellian distribution. Equations of motion were solved using the Taylor method of third order. The dynamical evolution was stopped at 300 fm/c and the fragments were identified with a clusterization procedure that recognizes the nucleons as a part of one fragment if their relative distance is less than a cutoff radius $r_c = 2.5$ fm. τ values do not change after 300 fm/c significantly, which allows a direct comparison with experimental values.

[1] R. W. Minich *et al.*, Phys. Lett. **B118**, 458 (1982).
[2] J. Finn *et al.*, Phys. Rev. Lett. **49**, 1321 (1982).
[3] M. E. Fisher, Physics **3**, 255 (1967).
[4] A. S. Hirsch *et al.*, Phys. Rev. C **29**, 508 (1984).
[5] A. D. Panagiotou *et al.*, Phys. Rev. Lett. **52**, 496 (1984).
[6] M. L. Gilkes *et al.*, Phys. Rev. Lett. **73**, 1590 (1984).
[7] J. Aichelin and X. Campi, Phys. Rev. C **34**, 1643 (1986).
[8] M. Mahi *et al.*, Phys. Rev. Lett. **60**, 1936 (1988).
[9] W. Bauer, Phys. Rev. C **38**, 1297 (1988).
[10] G. Peilert, H. Stocker, W. Greiner, A. Rosenhauer, A. Bohnet, and J. Aichelin, Phys. Rev. C **39**, 1402 (1989).
[11] N. T. Porile, A. J. Bujak, D. D. Carmony, Y. H. Chung, L. J. Gutay, A. S. Hirsch, M. Mahi, G. L. Paderewski, T. C. Sangster, R. P. Scharenberg, and B. C. Stringfellow, Phys. Rev. C **39**, 1914 (1989).
[12] S. J. Yennello *et al.*, Phys. Rev. C **41**, 79 (1990).
[13] S. J. Yennello *et al.*, Phys. Rev. C **48**, 1092 (1993).
[14] P. Kreutz *et al.*, Nucl. Phys. **A556**, 672 (1993)
[15] J. B. Elliot *et al.*, Phys. Lett. **B381**, 35 (1996).
[16] J. B. Elliot *et al.*, Phys. Lett. **B418**, 34 (1998).
[17] B. K. Srivastava *et al.* (EOS Collaboration), Phys. Rev. C **64**, 041605(R) (2001).
[18] R. P. Scharenberg *et al.* (EOS Collaboration), Phys. Rev. C **64**, 054602 (2001).
[19] B. K. Srivastava *et al.* (EOS Collaboration), Phys. Rev. C **65**, 054617 (2002).
[20] M. Kleine Berkenbusch, W. Bauer, K. Dillman, S. Pratt, L. Beaulieu, K. Kwiatkowski, T. Lefort, W.-C. Hsi, V. E. Viola, S. J. Yennello, R. G. Korteling, and H. Breuer, Phys. Rev. Lett. **88**, 022701 (2001).
[21] M. D'Agostino *et al.*, Nucl. Phys. **A650**, 329 (2004).
[22] B. Borderie *et al.*, Nucl. Phys. **A734**, 495 (2004).
[23] M. D'Agostino *et al.*, Nucl. Phys. **A724**, 455 (2004).
[24] S. Wang *et al.*, Phys. Rev. Lett. **74**, 2646 (1995).
[25] M. D'Agostino *et al.*, Nucl. Phys. **A650**, 329 (1999).
[26] J. B. Elliot *et al.*, Phys. Rev. C **62**, 064603 (2000).
[27] J. B. Elliot *et al.*, Phys. Rev. Lett. **88**, 042701 (2002).
[28] J. B. Natowitz *et al.*, nucl-ex/0206010.
[29] P. Chomaz and F. Gulminelli, Phys. Lett. **B447**, 221 (1999).
[30] W. Nörenberg, G. Papp, and P. Rozmej, Eur. Phys. J. A **14**, 43 (2002).
[31] Y. G. Ma *et al.*, Phys. Rev. C **69**, 031604(R) (2004).
[32] J. C. Pan, S. Das Gupta, and M. Grant, Phys. Rev. Lett. **80**, 1182 (1998).
[33] J. Pan and S. Das Gupta, Phys. Rev. C **57**, 1839 (1998).
[34] C. O. Dorso, V. C. Latora, and A. Bonasera, Phys. Rev. C **60**, 034606 (1999).
[35] M. Jandel *et al.*, J. Phys. G **31**, 29 (2005).
[36] V. Viola *et al.*, Nucl. Phys. **A681**, 267c (2001).
[37] R. Laforest *et al.*, Phys. Rev. C **59**, 2567 (1999).
[38] F. Gimeno-Nogues *et al.*, Nucl. Instrum. Methods Phys. Res. A **399**, 94 (1997).
[39] M. Veselsky *et al.*, Phys. Rev. C **62**, 064613 (2000).
[40] L. Tassan-Got, Nucl. Phys. **A524**, 121 (1991).
[41] A. S. Botvina, O. V. Lozhkin, and W. Trautmann, Phys. Rev. C **65**, 044610 (2002) (and references therein).
[42] A. S. Botvina, A. S. Iljinov, and I. N. Mishustin, Nucl. Phys. **A507**, 649 (1990).
[43] A. S. Botvina *et al.*, Nucl. Phys. **A475**, 663 (1987).
[44] X. Campi, Phys. Lett. **B208**, 351 (1988).

[45] X. Campi, J. Phys. A **19**, L917 (1986).
[46] Stauffer D, *Introduction to Percolation Theory* (Taylor and Francis, London, 1985).
[47] R. Ogul and A. S. Botvina, Phys. Rev. C **66**, 051601(R) (2002).
[48] N. Buyukcizmeci *et al*., Eur. Phys. J. A **25**, 57 (2005).
[49] H. Muller and B. D. Serot, Phys. Rev. C **52**, 2072 (1995).
[50] R. J. Lenk, T. J. Schlagel, and V. R. Pandharipande, Phys. Rev. C **42**, 372 (1990).